PENA CENDEKIA PUBLISHING
NURTURING IDEAS, ENRICHING KNOWLEDGE

Pena Journal of Flow Dynamics

Journal homepage:
https://penacendekia.com.my/index.php/pjfd/
ISSN: 3093-6802

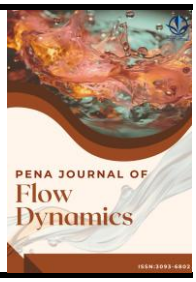

Simulation and Experimental Analysis of Laptop Air Multiplier Fan with Application of Coanda Effect

Cornelius Houben Christopher[1], Shirley Johnathan Tanjong[1,*]

[1] Department of Mechanical and Manufacturing Engineering, Faculty of Engineering, Universiti Malaysia Sarawak, 94300 Kota Samarahan, Sarawak, Malaysia

ARTICLE INFO

Article history:
Received 16 December 2024
Received in revised form 16 January 2025
Accepted 20 February 2025
Available online 31 March 2025

Keywords:
Simulation; Computational Fluid Dynamics; fan; air multiplier; Coanda effect; laptop cooling

ABSTRACT

This paper presents a simulation and experimental analyses of an air multiplier fan design as an alternative laptop cooling solution, using the application of Coanda effect. This study involved computer-aided design (CAD) and modelling of the designs using Autodesk Fusion360; fabrication of the proposed designs using fused deposition modelling (FDM) 3D printer; data collection of air velocity and sound level for the original equipment manufacturer (OEM) laptop fan and the 3D printed designs; computational fluid dynamic (CFD) simulation of the designs using ANSYS Fluent; and finally, validation and comparison of the data obtained from the experimental results to the simulation results. Important design characteristics were identified, such as using Eppler 473 as the airfoil profile, slit angle at 30^{o} and a slit width of 1 mm. Two concept designs, named Design 1 and Design 2, were generated based on these design characteristics. The air velocity and sound level experimental data were collected using the 3D printed prototype of Design 1 and Design 2, using an anemometer and a sound level meter, respectively. CFD simulation for Design 1 and Design 2 was done using ANSYS Fluent with standard *k*-epsilon as the turbulence model. The result obtained show that both conceptual designs outperformed the OEM fan based on air velocity and sound level generated. The airfoil surface generated an increase in air velocity due to the Coanda effect and the absence of rotating parts minimises noise.

1. Introduction

The advancements in semiconductors and other electronic components lead to more miniaturized computer components while also causing higher power consumption. It challenged the microelectronics industry to remove as much as 300 W/cm^2 of heat flux while maintaining temperature under 85^{o}C [12]. A conventional cooling system struggles to keep up with the cooling needed for the ever-increasing cooling load of newer electronic devices. The thermal design power of laptop central processing unit (CPU) processors declined in the past 10 years but then saw no change for the past 5 years which is 15W for low-end processors and 28W for high-end processors [20]. Centrifugal fan is the go-to option for many laptop manufacturers because of its high energy

* *Corresponding author.*
E-mail address: jtshirley@unimas.my

https://doi.org/10.37934/pjfd.1.1.2840

efficiency and suitability for application in small spaces. However, aerodynamic performance and noise of centrifugal fans have always been an issue [19]. Gaming laptops or workstation laptops generally use high thermal design power CPU processors. When working at maximum capacity, the centrifugal fan also operates at high revolutions per minute (RPM) to meet the requirement of the high cooling load. The frequency of tonal noise generated by centrifugal fan correlates directly with the rotation speed of the fan [13]. The noise generated by the centrifugal fan may often be perceived as distracting or annoying by users [18].

Bladeless fan, also known as an air multiplier fan, is similar to a centrifugal fan in which the surrounding air was induced into the fan to increase its airflow [9]. Bladeless fans are marketed as better fans because they provide steady airflow, increased airflow, and make less noise by reducing moving parts [8]. The term 'bladeless' refers to the lack of moving parts on the apparatus that emits airflow despite the design of a bladeless fan utilising an impeller, which is a centrifugal fan. Air multiplier fan uses the Coanda effect to draw more air from the atmosphere, resulting in increased airflow. Henri Coanda observed this phenomenon when his plane's engine burned before taking off in 1934 which led to extensive research on its practicality. Theodore von Karman later dedicated the new flow phenomenon name as Coanda effect in honour of Henri Coanda [1]. The Coanda effect simply describes a fluid tendency to move along a curved surface. The airfoil in the air multiplier fan design causes the Coanda effect to happen, creating an area of low pressure and ultimately drawing more air from the atmosphere.

The air multiplier fan is an interesting concept because it requires a centrifugal fan built-in by design to supply air that will undergo the Coanda effect. To integrate the concept of an air multiplier fan, the only critical component left is the airfoil design. Air multiplier fans produce less noise while generating more and even airflow using the help of the low-pressure area due to the air jet undergoing the Coanda effect. The conventional air multiplier fan has been the focus of recent studies [2,14] which yield some significant findings such as the optimal geometric design of an air multiplier fan. Yet, research on the air multiplier fan concept for cooling applications beyond the typical bladeless fan is scarce. The air multiplier concept on a miniaturised application and on tight spaces, such as on computer processors has also not been studied. Therefore, the main aim of this study was to analyse the performance of a small and conceptual design of the air multiplier fan in a laptop cooling application. To achieve the aim of the project, the objectives are detailed as follows:

i. To design and model the proposed air multiplier fan design using Autodesk Fusion360.
ii. To measure air velocity (unit in m/s) and sound level (unit in dBA) for the 3D printed models.
iii. To simulate the proposed design using ANSYS Fluent and to validate and compare the data obtained from the experimental results.

2. Background Review

2.1 Electronics Cooling System

There are numerous types of cooling systems used in an electronic system, such as conventional fan design, water-cooled design, microchannel cooling, and thermoelectric cooler. The conventional cooling system used for electronics is air cooling aided by a fan. With the proper design of the heat exchanger, conventional air cooling is capable of handling high cooling load. Previous research [6] had shown this to be effective by designing a universal heat exchanger capable of handling a maximum cooling load of 30W provided that the fluid used, air was cooled beforehand. However, a cooling system that utilises fan often encounters some problems namely in an enclosure. When the electronic components are considered, a huge performance drop in terms of static pressure and the

fan flow rate was observed using CFD with two different model types [11]. Different results might be shown with an electronic system that uses a proper heat sink system.

Liquid cooling had been proven to be better than conventional air cooling, which supports the increased thermal design power (TDP) of recent CPUs [7]. However, liquid cooling can be complicated when dealing with three-dimensional structures and electronics combined due to the need to distribute the cooling liquid evenly while avoiding leakages [17].

Thermoelectric cooler (TEC) allows heat to dissipate from the surface in contact via the Peltier effect and its thermal resistance can be controlled by the current flowing through TEC [5]. Microchannels on the other hand are a type of heat exchanger design suitable for high heat influx systems. Cong *et al.*, [5] designed a cooling system that uses TEC and a microchannel heat exchanger for a multi-chip electronic system. The combined system was able to utilise the maximum thermal management of a chip compared to when one of the TEC was not turned on.

2.2 Coanda Effect

Coanda effect is a phenomenon where a fluid jet tends to move along a convex surface. A simple demonstration of the Coanda effect can be done by holding the curvature of a spoon to running water from a tap, see Figure 1 [4]. The water from the tap which originally flow straight down has now changed its flow trajectory following the curvature of the spoon. Coanda effect hysteresis is a term to explain different fluid jet behaviour which depends on the surface angle and deflection when the fluid jet is undergoing the Coanda effect [16]. The fluid jet would either stay attached to the Coanda surface or deviate from the surface with a visible separation bubble. It was also found that for cases where free air flow and jet attachment are visible, the Reynolds number of jet flow and values for critical flow attachment and detachment angle are inversely proportional [15]. Extended Coanda effect describes the tendency of the fluid jet that has undergone the Coanda effect to reattach to the convex or concave surface after impinging occurs [10]. A commonly known application of Coanda effect is the bladeless fan or the air multiplier fan (see Figure 2).

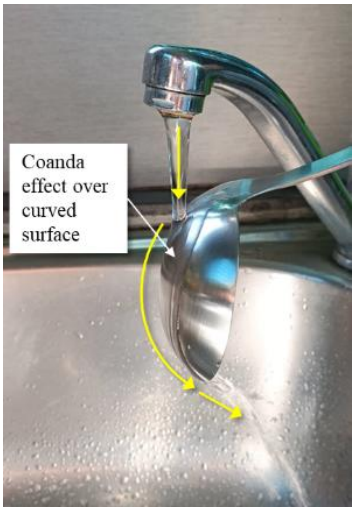

Fig. 1. Demonstration of the Coanda effect where water flow follows the curvature of the spoon.

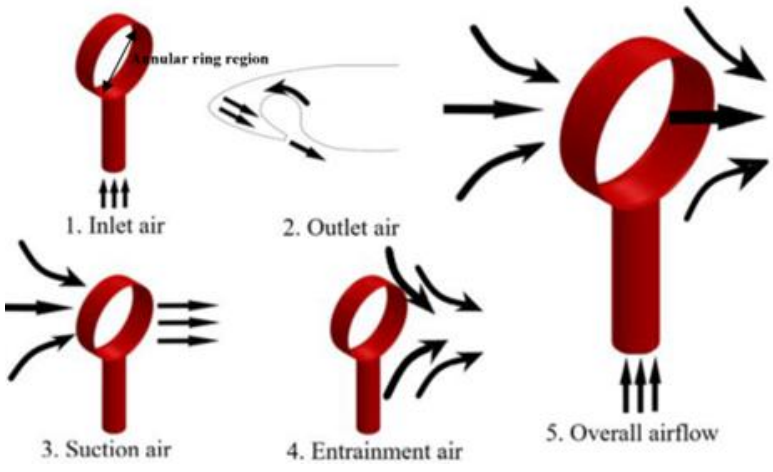

Fig. 2. Airflow motion of a commercial air multiplier fan [14].

2.3 Air Multiplier Fan Design Characteristics

Multiple designs use the Coanda effect as flow manipulation method. Aslam *et al.,* [3] proposed fan design based on Eppler 473 airfoil (see Figure 3) because the airfoil is commonly used for low-speed and low-Reynolds number applications [3]. Eppler 473 airfoil profile was selected as the bladeless fan cross-section design as it has good curvature, symmetry geometry and a flat upper surface. Ravi and Rajagopal [14] concluded that Eppler 473 airfoil profile exhibits better air discharge ratio than Eppler 169 and Eppler 479 (see Figure 4).

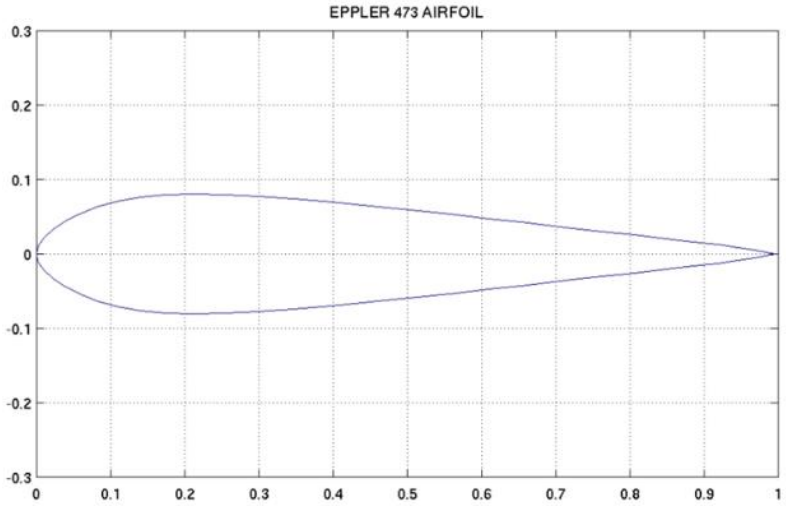

Fig. 3. Eppler 473 Airfoil profile characteristic

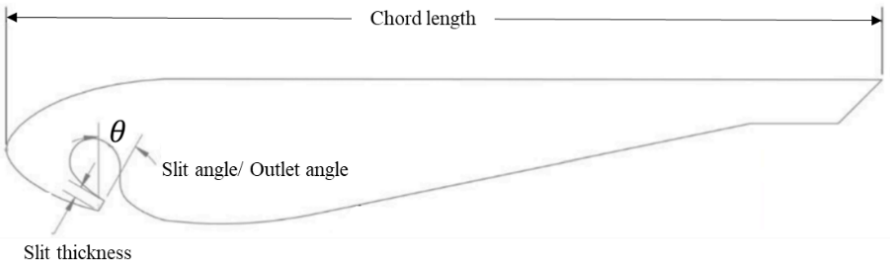

Fig. 4. Optimal design parameters of bladeless fan in Ref. [14]: Eppler 473 profile, chord length 100 mm, slit thickness 1mm, hydraulic diameter 300mm and slit angle 80.

3. Methodology

The research consists of 2 main data acquisition methods, i.e. experimental and simulation approaches. Experimental works were prioritised as the experimental data was used to validate the simulation data.

3.1 Design of Air Multiplier Fan

Based on past research on the cross-sectional profile of the bladeless fan, Eppler 473 was found to be the most suitable option to provide the maximum air discharge ratio compared to other aerofoil profiles. The proposed designs, Design 1 and Design 2 were designed and modelled using the

geometric features of an air multiplier fan, details in Table 1. Design 1 uses two aerofoils in an oval shape, while Design 2 uses only one aerofoil that forms a slit on the bottom of a laptop.

Table 1
Geometric features of Design 1 and Design 2

Feature	Design 1	Design 2
Aerofoil profile	Eppler 473	Eppler 473
Slit angle	30^o	30^o
Slit thickness	1mm	1mm
Cross-sectional shape	Oval, double profile	Single profile
Height of cross-section	30 mm	20 mm
Chord length	50 mm	50 mm
Inner diameter	6.2 mm	-

The design characteristics of the fan were decided based on past research by Ravi and Rajagopal [14] and Jafari *et al.,* [9] with the dimension limitation of the laptop in consideration. Although Ravi and Rajagopal [14] concluded that the discharge ratio increases with slit angle however slit angle of 30^o was chosen as it was easier to design with and provided satisfactory performance. Figure 5(a)-(b) and Figure 6(a)-(b) shows the isometric view and cross-section view of each design.

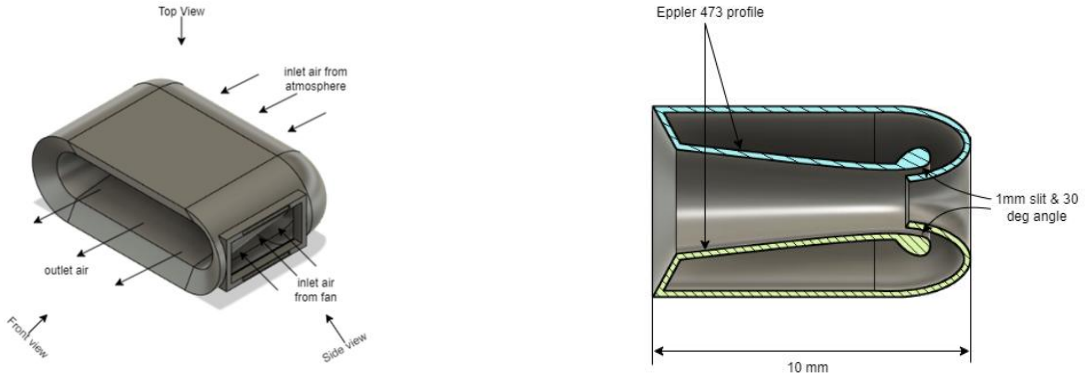

(a) (b)

Fig. 5. View (a) Isometric view of Design 1 (b) Cross-section view of Design 1

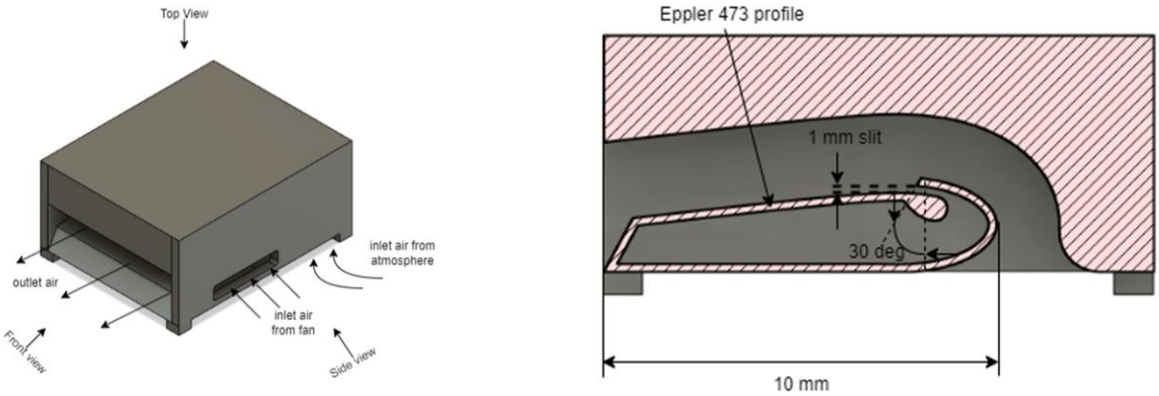

(a) (b)

Fig. 6. View (a) Isometric view of Design 2 (b) Cross-section view of Design 2

3.2 Experimental Data Collection

The air multiplier fan design was modelled in Autodesk Fusion 360 which supports the visualization of the DAT file of the Eppler 473 aerofoil profile with the help of add-ons. Subsequently, the 3D model was sliced using Creality Slicer and 3D printed using the Ender 5 Plus 3D printer with PETG filament. For experimental data collection, the designs were assembled with parts as shown in Figure 7(a) and (b). The attached parts were also 3D printed using PETG filament.

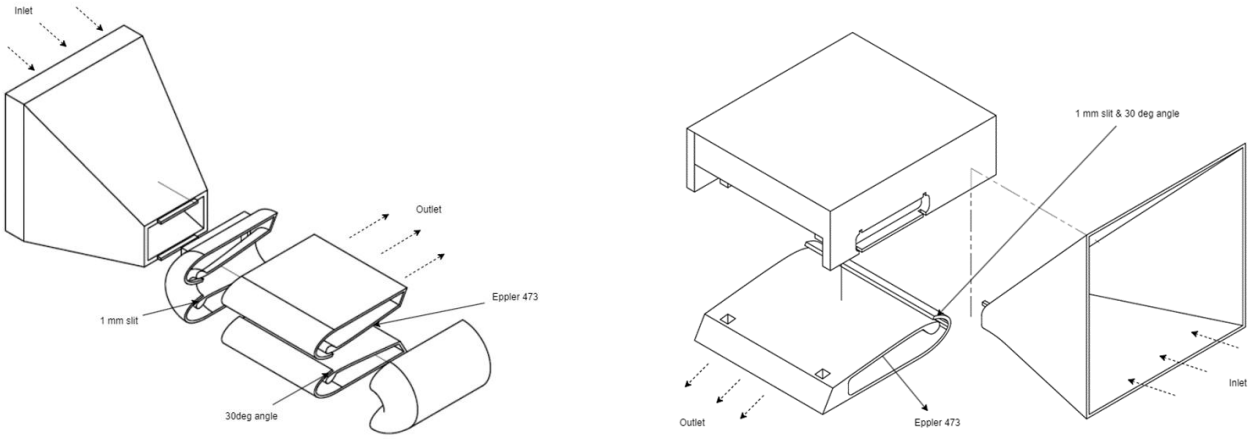

(a) (b)

Fig. 7. Assembly (a) Design 1 assembly for experimental data collection (b) Design 2 assembly for experimental data collection

Two variables were collected to compare the design, i.e. air velocity and sound level. Air velocity was measured using a UNI-T UT363BT mini anemometer and the sound level was measured using a UNI-T UT363BT sound level meter. Both devices have Bluetooth connection capability which allows wireless data recording. To measure air velocity, the anemometer was placed at 0 cm from the outlet air jet path. The sound level for both designs were measured at 2 distances (placement of sound meter). In the first set of data, sound was measured at 0 cm from the outlet air jet path. In the second set of data, sound as measured at 30 cm distance from the outlet air jet path. The 30 cm distance was to simulate noise coming from the computer fan perceived by a user.

3.3 Turbulence Model

The designs were modelled in 3D using Fusion 360 and exported to ANSYS Modeller. CFD simulation in Ansys ran using the standard $k-\varepsilon$ model. The standard $k-\varepsilon$ model is built based on the model transport equation of turbulence kinetic energy (k) and the dissipation rate (ε). The transport equation used to derive the turbulence kinetic energy (k) and the dissipation rate (ε) are as follows (ANSYS Inc, 2009):

$$\frac{\partial}{\partial t}(\rho k)+\frac{\partial}{\partial x_i}(\rho k u_i)=\frac{\partial}{\partial x_j}\left[\left(\mu+\frac{\mu_t}{\sigma_t}\right)\frac{\partial k}{\partial x_j}\right]+G_x+G_b-\rho\epsilon-Y_M+S_k \quad (1)$$

$$\frac{\partial}{\partial t}(\rho \epsilon)+\frac{\partial}{\partial x_i}(\rho \epsilon u_i)=\frac{\partial}{\partial x_j}\left[\left(\mu+\frac{\mu_t}{\sigma_\epsilon}\right)\frac{\partial \epsilon}{\partial x_j}\right]+C_{1\epsilon}\frac{\epsilon}{k}(G_k+C_{3\epsilon}G_b)-C_{2\epsilon}\rho\frac{\epsilon^2}{k}+S_\epsilon \quad (2)$$

where; G_k: generation of kinetic energy due to velocity gradients
G_b: generation of kinetic energy due to buoyancy
Y_M: fluctuating dilation in compressible turbulence to the dissipation rate

$$\mu_t = \rho C_\mu \frac{k^2}{\epsilon} \tag{3}$$

The values of the constants used are: $C_{1\epsilon} = 1.44$, $C_{2\epsilon} = 1.92$, $C_\mu = 0.09$,and the turbulent Prandtl number for k and ϵ are $\sigma_k = 1.0$ and $\sigma_\epsilon = 1.3$.

3.4 Meshing and Boundary Conditions

In ANSYS, the cooling system was simulated in 3D and some geometry modifications are done. To mesh the model, element sizing is used to refine the mesh shape and element size on the critical components of the model such as near the body of the fan. The skewness graph in the mesh quality setting can be used to determine the quality of the mesh. If the graph skews to the left, this means that the mesh quality is good and vice versa for the right-skewed graph. After the desired quality of the mesh is obtained, the process continued with defining the boundary condition. Boundary conditions such as the inlet, walls and outlet are specified and given an initial known value. The simulation setup for mesh and boundary conditions for both designs are: face sizing method, element size of 0.0015 m, initial air velocity of 2 m/s and 5% turbulent intensity (moderate turbulence).

4. Results and Discussion

4.1 Experimental Data

4.1.1 Air velocity

Air velocity measurements were recorded in an enclosed room with stagnant airflow for 1.5 minutes with a delay of 1s between each data was recorded, thus total number of measurements, $N = 90$. Figure 8 and Table 2 summarise the distribution of measurements (90 readings) for each fan type.

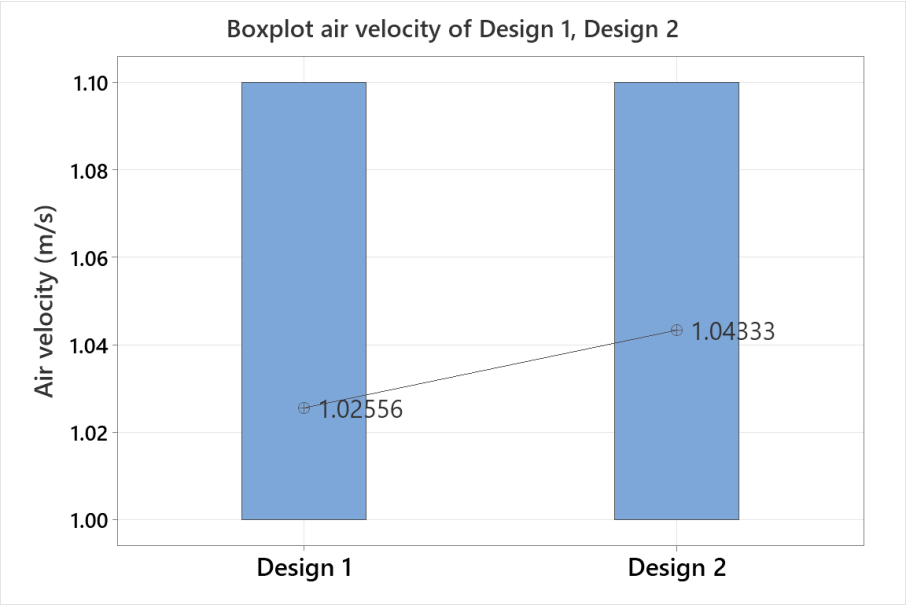

Fig. 8. Boxplot of air velocity measurements

Table 2
Descriptive statistics of air velocity measurement

Variable	Design 1	Design 2
N	90	90
Mean	1.0256	1.0433
Standard deviation	0.0439	0.0498
Minimum	1.00	1.00
Median	1.00	1.00
Maximum	1.10	1.10

As shown in Figure 8 and Table 2, the mean outlet air velocity of each design was 1.03 m/s (Design 1) and 1.04 m/s (Design 2). The performance of Design 1 and 2 are similar with mean difference of approximately 0.01 m/s. During the design stage, it was assumed that Design 1 will perform better than Design 2 in displacing air due to the double-profile, hence larger slit surface area present in Design 1. During data collection, it was observed that there was backflow from the wind source which was caused by the shape of the air intake funnel. The scope of this study does not cover the most optimal funnel geometry as the external fan for providing air velocity was simply used as a proxy for the actual fan used in the simulation. The backflow reduced air flow through the inlet of Design 1 and 2, affecting the significance of the slit surface area on outlet air velocity.

4.1.2 Sound level

Sound level data was collected in an anechoic room and no external loud noise sources were present during data collection. Measurements were conducted in 1.5 minutes with a delay of 1s between each data, thus total number of measurements, $N = 90$. For measurement of sound level at distance 0 cm, the control data was also collected, to provide as a baseline when no fan operates. Figure 9 and 10 show the time plot of sound level measured at distance 0 cm and 30 cm. Table 3 and 4 summarise the distribution of measurements for each design and the OEM fan type.

Referring to Table 3, at 0 cm, Design 1 and Design 2 exhibit similar sound level i.e. within the range of 47.9 - 49.7 dBA (Design 1) and 47.6 - 51.1 dBA (Design 2) and means of 48.7 dBA and 48.2 dBA, respectively. The OEM fan showed a larger range (46.6 - 52.5dBA) compared to Design 1 and 2, as shown in Figure 9. During data collection, the OEM fan was observed to fluctuate between speeds of 2700 RPM, 3000 RPM and 3200 RPM which corresponds to 48dBA, 50dBA and 52 dBA respectively. It is impossible to set the angular speed of a laptop's fan to a constant number as the system constantly adjusting the fan speed according to the load experienced by the CPU. Even though no programmes were running, the laptop's fan speed fluctuates from time to time. This may be caused by some background processes running required by the operating system. Figure 10 and Table 4 show the sound level measured at 30cm distance from the outlet. The OEM fan exhibited higher mean sound level of 44.2dBA as compared to Design 1 and Design 2, at 43.8 dBA and 42.9 dBA, respectively.

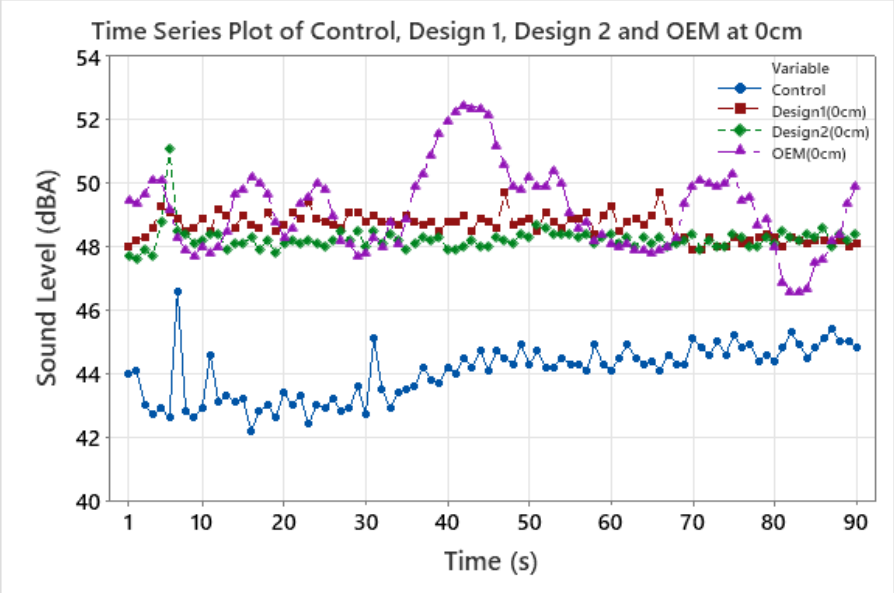

Fig. 9. Time plot of sound level measurements at 0 cm distance from outlet

Table 3
Descriptive statistics of sound level measured at 0 cm

Variable	Control	OEM	Design 1	Design 2
N	90	90	90	90
Mean	44.032	49.184	48.654	48.231
Standard deviation	0.867	1.343	0.398	0.378
Minimum	42.2	46.6	47.9	47.6
Median	44.25	49.15	48.7	48.2
Maximum	46.6	52.5	49.7	51.1

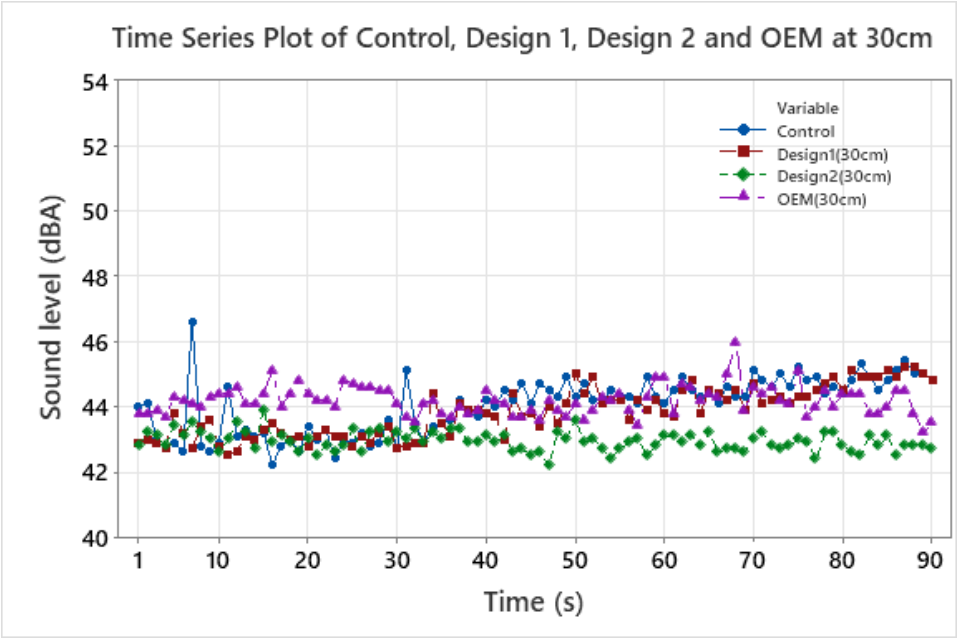

Fig. 10. Time plot of sound level measurements at 30 cm distance from outlet

Table 4
Descriptive statistics of sound level measured at 30 cm

Variable	OEM	Design 1	Design 2
N	90	90	90
Mean	44.194	43.823	42.927
Standard deviation	0.438	0.752	0.295
Minimum	43.2	42.5	42.2
Median	44.2	43.8	42.9
Maximum	46	45.2	43.9

4.2 Simulation Data

Figure 11(a)-(b) show the contour result of air velocity gradient obtained using ANSYS Fluent. It can be observed that Design 1 outlet streamline was linear compared to Design 2 demonstrates a downward streamline. This is consistent with the Coanda effect, such that in Design 2, the airflow is attached to the side of the outlet.

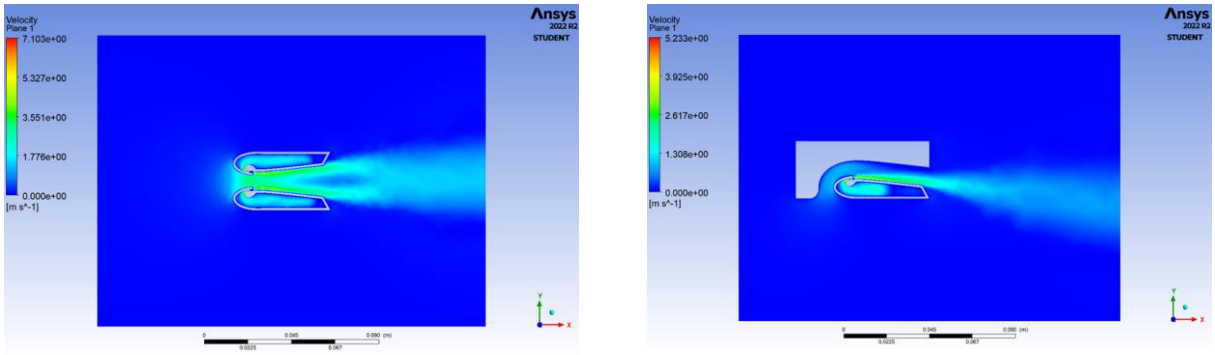

(a) (b)

Fig. 11. Contour (a) Contour results of air velocity for Design 1 (b) Contour results of air velocity for Design 2

Figure 12 shows the outlet air velocity versus distance. Figure 12(b) shows that Design 1 has peak velocity at 1.51 m/s, at 15-20 mm, then maintains a velocity of 1.4 – 1.5 m/s within the 20-70 mm distance. Design 2 highest velocity is at of 1.10 m/s at 0 mm, then declines as distance increases. Figure 12(a) magnifies the plot when only the first 10 mm distance is highlighted, which gives a mean velocity of 1.104 m/s for Design 1 and 0.965 m/s for Design 2.

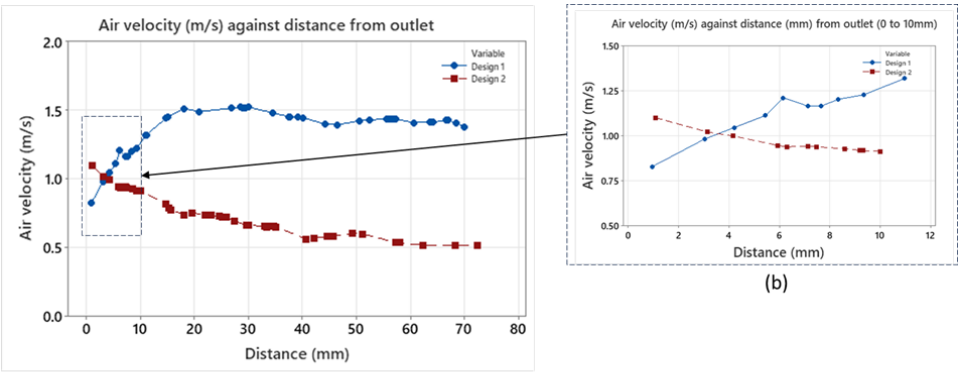

(a) (b)

Fig. 12. Comparison of outlet air velocity between Design 1 and 2: (a) Plot at distance 0-70 mm from the outlet; (b) plot magnified for distance < 10 mm from the outlet

4.3 Summary on Results

To summarise, Design 1 is the superior fan choice based on the findings obtained from the experimental and simulation data. In the simulation, the mean air velocity 10mm from the opening was 1.104 m/s and 0.965 m/s for Design 1 and 2, respectively. The simulation data provided more insight into which design performed better as more precise result can be obtained. In the experimental data, Design 1 and Design 2 performed similarly on the air velocity aspect which were 1.03 m/s and 1.04 m/s respectively. To calculate percentage difference between the experimental and simulation results, the percentage results are calculated by taking the simulation result as baseline, calculated as follows:

$$Percentage\ difference, \Delta = \left|\frac{Simulation\ result - Experimental\ result}{Simulation\ result}\right| \times 100\% \quad (4)$$

For air velocity, v, the percentage difference, $\Delta v_{Design\ 1} = 6.7\%$ and $\Delta v_{Design\ 2} = 7.8\%$

No significant difference in terms of sound level for both Design 1 and 2, with mean of 48.7 dBA and 48.2 dBA m, measured at 0 cm, respectively. Nevertheless, experimental data suggests that both designs perform better in minimising noise as compared to the OEM fan. At 30 cm distance from the fan, the sound level decreases to 43.82 dBA and 42.93 dBA respectively which makes the difference negligible to human hearing.

5. Conclusions

The main aim of this study was to analyse the performance of a small and conceptual design of the air multiplier fan for laptop cooling solution. The proposed design focused on the application of air multiplier fan leveraging the Coanda effect to improve air displacement with minimal moving parts. Two designs were proposed, both utilising the aerofoil profile (Eppler 473), slit angle (30^{o}) and slit thickness (1mm). Design 1 employs a double-profile aerofoil cross-sectional area, while Design 2 employs a single-profile variant. Both designs were 3D printed using the Ender 5 Plus 3D printer with PETG filament. The 3D printed models were used for experimental data collection. Design 1 and Design 2 performed similarly on the air velocity aspect, with an average 1.03m/s to 1.04 m/s, respectively. On sound level, Design 1 and Design 2 performed better than the 49.2 dBA OEM fan at 0 cm distance from the fan, with lower sound level measured at a mean of 48.7 dBA and 48.2 dBA, respectively. However, the sound level at 30cm distance for Design 1, 2 and the OEM fan was comparable to the control data. A human user would not notice the difference in noise from the Design 1 and 2 if similar conditions were replicated. It was determined that the main source of the noise generated was mechanical noise generated by the supplying fan and not aerodynamic noise expected from the bladeless fan design. Several limitations and opportunities for further work were identified during the execution of the research. Firstly, the fabricated models were not smooth due to the limitations of an FDM process. Therefore, alternative fabrication processes such as selective laser sintering (SLS) or stereolithography (SLA) 3D printing are recommended for future works. Secondly, the analysis on the proposed designs can be expanded by testing other parameters to compare the air multiplier fan and OEM fan, such as temperature and vibration. Lastly, different types of build material of the design can be investigated to optimise the design as a better cooling solution for computer processors.

Acknowledgement
We hereby acknowledge that we conducted this research at the Universiti Malaysia Sarawak without any external funding. We are grateful for the support and resources provided by the university, which enabled us to conduct this research. The university's facilities, expertise, and academic environment played a crucial role in the successful completion of our project.

References

[1] Ahmed, Noor A. *Coanda effect: flow phenomenon and applications*. CRC Press, 2019. https://doi.org/10.1201/9780429441240

[2] Akgöl, Doğukan, and Şahin Yavuz. "Influence of geometric parameters on the average outlet velocity of the bladeless fan." *Avrupa Bilim ve Teknoloji Dergisi* 28 (2021): 1501-1507. https://doi.org/10.31590/ejosat.1022116

[3] Aslam, Haseeb, Muhammad Zulqarnain Arif, Majid Ali, and Adeel Javed. "Design and CFD analysis of bladeless ceiling fan." In *2021 International Bhurban Conference on Applied Sciences and Technologies (IBCAST)*, pp. 782-787. IEEE, 2021. https://doi.org/10.1109/IBCAST51254.2021.9393254

[4] Camuffo, Dario. *Microclimate for cultural heritage: Measurement, risk assessment, conservation, restoration, and maintenance of indoor and outdoor monuments*. Elsevier, 2019. https://doi.org/10.1016/B978-0-444-64106-9.00001-8

[5] Cong, Bo, Yanmei Kong, Yuxin Ye, Ruiwen Liu, Xiangbin Du, Lihang Yu, Shiqi Jia, Zhiguo Qu, and Binbin Jiao. "A combined solution of thermoelectric coolers and microchannels for multi-chip heat dissipation with precise temperature uniformity control." *Applied Thermal Engineering* 219 (2023): 119370. https://doi.org/10.1016/j.applthermaleng.2022.119370

[6] Doubek, Martin, and Václav Vacek. "Universal heat exchanger for air and evaporative cooling of electronics." *Thermal Science and Engineering Progress* 23 (2021): 100865. https://doi.org/10.1016/j.tsep.2021.100865

[7] Fan, Yuehong, Casey Winkel, Devdatta Kulkarni, and Wenbin Tian. "Analytical design methodology for liquid based cooling solution for high TDP CPUs." In *2018 17th IEEE Intersociety Conference on Thermal and Thermomechanical Phenomena in Electronic Systems (ITherm)*, pp. 582-586. IEEE, 2018. https://doi.org/10.1109/ITHERM.2018.8419562

[8] Gammack. P. D., Nicolas, F. and Simmonds, K. J. (2012). Fan. United States Patent No. US008308445B2.

[9] Jafari, Mohammad, Hossein Afshin, Bijan Farhanieh, and H. Bozorgasareh. "Numerical aerodynamic evaluation and noise investigation of a bladeless fan." *Journal of Applied Fluid Mechanics* 8, no. 1 (2014): 133-142. https://doi.org/10.36884/jafm.8.01.21872

[10] Li, Angui. "Extended Coanda Effect and attachment ventilation." *Indoor and Built Environment* 28, no. 4 (2019): 437-442. https://doi.org/10.1177/1420326X19833850

[11] Manaserh, Yaman M., Mohammad I. Tradat, Cong Hiep Hoang, Bahgat G. Sammakia, Alfonso Ortega, Kourosh Nemati, and Mark J. Seymour. "Degradation of fan performance in cooling electronics: experimental investigation and evaluating numerical techniques." *International Journal of Heat and Mass Transfer* 174 (2021): 121291. https://doi.org/10.1016/j.ijheatmasstransfer.2021.121291

[12] Murshed, SM Sohel, ed. *Electronics cooling*. BoD–Books on Demand, 2016. https://doi.org/10.5772/63321

[13] Ottersten, M., H. D. Yao, and L. Davidson. "Inlet gap effect on aerodynamics and tonal noise generation of a voluteless centrifugal fan." *Journal of Sound and Vibration* 540 (2022): 117304. https://doi.org/10.1016/j.jsv.2022.117304

[14] Ravi, Dineshkumar, and Thundil Karuppa Raj Rajagopal. "Numerical investigation on the effect of geometric shape and outlet angle of a bladeless fan for flow optimization using CFD techniques." *International Journal of Thermofluids* 15 (2022): 100174. https://doi.org/10.1016/j.ijft.2022.100174

[15] Skotnicka-Siepsiak, Aldona. "The applicability of coanda effect hysteresis for designing unsteady ventilation systems." *Energies* 14, no. 1 (2020): 34. https://doi.org/10.3390/en14010034

[16] Soleimanikutanaei, Soheil, Cheng-Xian Lin, Nezih Pala, and Gang Quan. "Performance Evaluation of Liquid 3D Chip Cooling Systems Under Non-Uniform Power Density: Effects of Inlet and Plenum Configurations." In *2019 18th IEEE*

Intersociety Conference on Thermal and Thermomechanical Phenomena in Electronic Systems (ITherm), pp. 1260-1265. IEEE, 2019. https://doi.org/10.1109/ITHERM.2019.8757340

[17] Sommerfeldt, Scott D., and Kent L. Gee. "Active control of axial and centrifugal fan noise." In *Proceedings of Meetings on Acoustics*, vol. 19, no. 1. AIP Publishing, 2013. https://doi.org/10.1121/1.4799648

[18] Wang, Jiahao, Xiaomin Liu, Chenye Tian, and Guang Xi. "Aerodynamic performance improvement and noise control for the multi-blade centrifugal fan by using bio-inspired blades." *Energy* 263 (2023): 125829. https://doi.org/10.1016/j.energy.2022.125829

[19] Zhou, Guohui, Ji Li, and Zizhou Jia. "Power-saving exploration for high-end ultra-slim laptop computers with miniature loop heat pipe cooling module." *Applied Energy* 239 (2019): 859-875. https://doi.org/10.1016/j.apenergy.2019.01.258

[20] UIUC Applied Aerodynamics Group. *UIUC Airfoil Coordinates Database*. Retrieved July 7, 2022